JOC The Journal of Organic Chemistry

pubs.acs.org/joc Article

Self-Assembly of Functionalized Lipophilic Guanosines into Cation-Free Stacked Guanine-Quartets

Marilena Campitiello, Alessio Cremonini, Marco A. Squillaci, Silvia Pieraccini, Artur Ciesielski, Paolo Samorì,* and Stefano Masiero*

Cite This: J. Org. Chem. 2021, 86, 9970–9978 Read Online

ACCESS | Metrics & More | Article Recommendations | Supporting Information

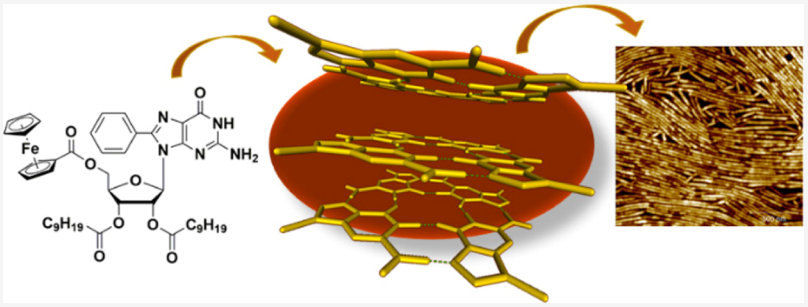

ABSTRACT: The hierarchical self-assembly of various lipophilic guanosines exposing either a phenyl or a ferrocenyl group in the C(8) position was investigated. In a solution, all the derivatives were found to self-assemble primarily into isolated guanine (G)-quartets. In spite of the apparent similar bulkiness of the two substituents, most of the derivatives form disordered structures in the solid state, whereas a specific 8-phenyl derivative self-assembles into an unprecedented, cation-free stacked G-quartet architecture.

INTRODUCTION

Among DNA bases, guanine (G) exhibits a unique ability to undergo self-assembly, forming various distinct supramolecular structures.[1,2] In particular, lipophilic guanosine derivatives have been reported to generate either supramolecular ribbon-like architectures[3−6] or tetrameric array (G-quartets)-based assemblies.[7,8] The formation of a specific assembly motif is ruled by both the specific chemical structure of the derivative[9,10] and the environmental conditions.[10,11] Among various G assemblies, G-quartet (hereafter G_4)-based supramolecular architectures are by far the most important because of the biological relevance of this structural motif in DNA.[12,13] Many G_4-based lipophilic complexes can be found in the literature, ranging from octamers (two stacked G_4s) and hexadecamers,[14−16] these being the most frequent and studied examples, up to pseudopolymeric stacked assemblies.[17] All these aggregates form spontaneously only in the presence of a metal cation, with the latter playing a crucial role in templating and stabilizing these architectures. For this reason, simple, isolated G_4s are probably the least-described supramolecular structures that originate from guanosine because, in the absence of templating cations, the common self-assembled motif of lipophilic guanosines has a ribbon-like architecture. Isolated G_4s as the main species, either in the absence[18−21] or in the presence[22,23] of a metal cation, have been indeed seldom reported. Isolated G_4s lacking a templating ion are observed when a bulky substituent is placed at the C(8) position of the nucleobase or, more generally, in cases where the formation of G-ribbons is hindered by the molecular structure. The ability of isolated G_4s, in the absence of a templating cation, to form higher-order organized assemblies has never been reported.

Here, we have focused our attention on both 8-ferrocenyl and 8-phenyl functionalized lipophilic guanosines carrying groups with different bulkiness at the 5′ position (Scheme 1), and we show that subtle modifications in the molecular structure cause a dramatic change in the propensity of the molecules to undergo a hierarchical self-assembly. In particular,

Scheme 1. Chemical Structures of the Investigated Guanosine Derivatives

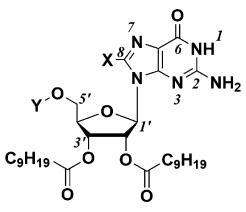

1 (8Ph5Fc)	X = Ph, Y = CO-Fc
2 (8Ph5OH)	X = Ph, Y = H
3 (8Ph5Si)	X = Ph, Y = TBDMS
4 (8Ph5C10)	X = Ph, Y = CO-C_9H_{19}
5 (8Fc5C10)	X = Fc, Y = CO-C_9H_{19}
6 (8Fc5Si)	X = Fc, Y = TBDMS
7 (8Fc5OH)	X = Fc, Y = H
8 (8Fc5Ph)	X = Fc, Y = CO-Ph

Received: March 2, 2021
Published: July 19, 2021

https://doi.org/10.1021/acs.joc.1c00502
J. Org. Chem. 2021, 86, 9970−9978

lipophilic guanosine derivative **1** (**8Ph5Fc**) was found to form isolated G_4s, which further self-assemble into stacked cation-free architectures. Conversely, derivatives **2**−**8**, and derivative **8** (**8Fc5Ph**) especially, where phenyl and ferrocenyl substituents are swapped with respect to **1**, exhibit no clear tendency to form supramolecular assemblies arising from piling up of G_4s.

RESULTS AND DISCUSSION

All investigated G derivatives were synthesized, starting from commercial guanosine, as described in Schemes S1−S4.

The circular dichroism (CD) spectrum of all compounds in CH_2Cl_2 shows only a weak molecular induced circular dichroism (ICD) band, attributed to the chiral perturbation of the guanine chromophore by the chiral sugar residue, and does not change upon the addition of either MeOH or [2.2.2] cryptand: this rules out the presence of templating ions residual from synthetic procedures. In contrast, deliberate addition of KI produces a strong excitonic spectrum, characteristic of G_4 stacking[24] (Figure S1).

A typical feature of the ^{1}H-NMR spectra of G_4 structures is the splitting of the signal for exocyclic amino protons into two signals as hydrogen bonding produces a large downfield shift of the proton involved in G_4 formation.[16] Usually, this signal splitting is not observed at room temperature because the two protons are in fast exchange regime, but it can be easily monitored by lowering the temperature. Figures S2−S9 show the downfield portion of the ^{1}H-NMR spectrum of the investigated compounds in CD_2Cl_2 at different temperatures in the absence of added metal cations. In all cases, signals that can be ascribed to amino groups start to appear at −5 to −20 °C both in the 9−10 ppm and in the 5−5.5 ppm ranges, and they become progressively sharper upon further lowering the temperature. In the case of **8Ph5Fc** (Figure S2), the amino proton signal is baseline-broadened in the CD_2Cl_2 room temperature spectrum. At −5 °C, two signals start to appear at 9.8 and 5.5 ppm for bound-N(2)H and free-N(2)H, respectively, and they shift slightly downfield and upfield, respectively, by further lowering the temperature. Moreover, the N(1)H imino proton signal resonates at 12.6 ppm at room temperature and undergoes deshielding upon lowering the temperature. The same signal resonates at 10.9 ppm in dmso-d_6, suggesting that in CD_2Cl_2, G is H-bonded already at room temperature. All the other investigated compounds show the same behavior, yet they differ in two aspects. First, the two amino signals start to appear only at lower temperatures (compare −20 °C spectra shown in Figures S2−S9). Second, imino and amino signals of the second assembled species (e.g., 12.38 and 9.98 ppm for **8Fc5C10**, Figure S6) become visible in most cases (with the exception of the two 5'OH derivatives **8Ph5OH** and **8Fc5OH**, see below) in the downfield portion of the spectrum. No clear evidence could be obtained on the architecture of these minor species. Nonetheless, this suggests a higher stability for the aggregate formed by **8Ph5Fc**, while for derivatives **2**−**8**, other, although minor, self-assembly pathways are viable.

Further evidence of the existence of self-assembled species in solution is given by nuclear Overhauser effect (NOE) spectra (Figures 1 and S10−S16). As the first general observation, in all cases, NOE spectra display cross-peaks having the same phase as the diagonal. This feature is characteristic of a slow tumbling regime, implying that the objects in the solution have a molecular weight above ca. 2000 Da,[25] whereas the molecular

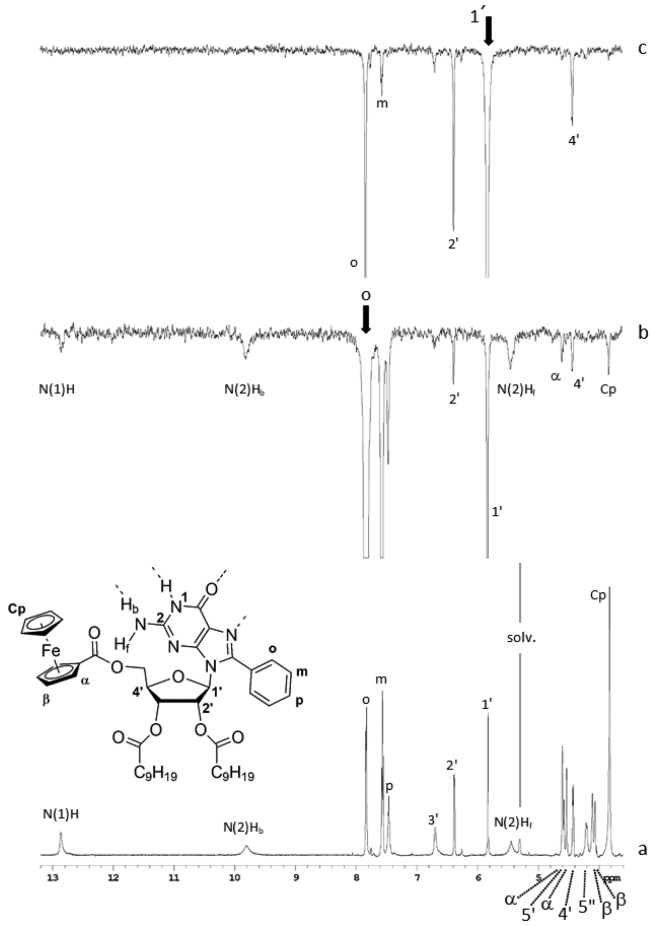

Figure 1. (a) Downfield portion of the 600 MHz ^{1}H-NMR spectrum of **8Ph5Fc** in CD_2Cl_2 (4.3 mM) at −20 °C and signal assignment (diastereotopic protons were not assigned); (b) NOESY-1D spectrum of the same sample upon irradiation at 7.83 ppm ("*o*" protons); (c) NOESY-1D spectrum of the same sample upon irradiation at 5.82 ppm (1′ proton). In each NOE spectrum were used 512 coadded transients, a recycle delay of 0.6 s, a mixing time of 0.6 s, and a 50 Hz shaped pulse. Irradiated frequencies are indicated with an arrow.

weight of an isolated molecule of **1**−**8** falls in the range of 667−929 Da. Another common feature of the main species formed by all of the investigated compounds is their preference for the *syn* conformation around the glycosidic bond. Figure 1b,c shows selected one-dimensional NOE spectroscopy (1D-NOESY) spectra of **1** recorded at −20 °C as an example. The interaction between "*o*" and H1' protons, already strong at room temperature (not shown), and the absence of any correlation between H5'/H5" and phenyl protons points to an exclusive *syn* conformation for **1**, as depicted in the inset of Figure 1a. Spectra reported in Figures S10−S16 point to the same conclusion. In the case of derivatives **8Ph5OH** and **8Fc5OH**, lacking a bulky substituent at the 5′ position, the *syn* conformer is possibly stabilized by an intramolecular H-bond between 5'OH and N(3) (see spectrum d in Figure S10).

It is known[26] that a downfield shift of the ribose H2' proton parallels an increase in the percentage of *syn* conformer population. In particular, 8-bromoguanosine ($\delta_{H2'}$ = 5.01 ppm in DMSO-d_6) is ca. 90% *syn*, while guanosine ($\delta_{H2'}$ = 4.429 ppm) is only 40% *syn*. Although a direct comparison with these figures is not possible, an analysis of the observed chemical shifts for derivatives **1**−**8** (see Table S1) allows some

https://doi.org/10.1021/acs.joc.1c00502
J. Org. Chem. 2021, 86, 9970−9978

qualitative conclusions. The introduction of ferrocenyl substituent at the 8-position exhibits a marked effect on the chemical shift of both H1' and H2' sugar protons, which move downfield by about 1 ppm. On the other hand, the 8-phenyl substituent exhibits a smaller effect and is limited to the H2' and H3' protons. Taking this result into account, it is possible to notice that the H2' proton tends to resonate at lower fields than H1' for the 8-phenyl derivatives, while 8-ferrocenyl derivatives show the same chemical shift order ($\delta_{H1'} > \delta_{H2'} > \delta_{H3'}$) as the reference compounds (entries **h**−**n** in Table S1). This suggests that the phenyl ring has a higher ability to drive the conformational equilibrium toward the *syn* isomer than the ferrocenyl substituent. In particular, the unique sequence $\delta_{H3'} > \delta_{H2'} > \delta_{H1'}$ shown by **8Ph5Fc** in CD_2Cl_2 should be noticed.

NOE spectra also provide unambiguous information on the structure of the main self-assembled species in solution. Another feature common to the main species formed by **1**−**8** is the dipolar coupling between the protons of the substituent at the C(8) position and the exocyclic amino group. For example, in the case of **8Ph5Fc**, the *o* protons interact with both exocyclic amino and ferrocene protons (Figure 1b). These proximities can only occur at the intermolecular level and rule out G-ribbon assemblies (see Figure S17) but point to a G_4 structure (such as the one presented in Figure 2 in the case of **8Ph5Fc**) as the main self-assembled aggregate formed by all the derivatives.

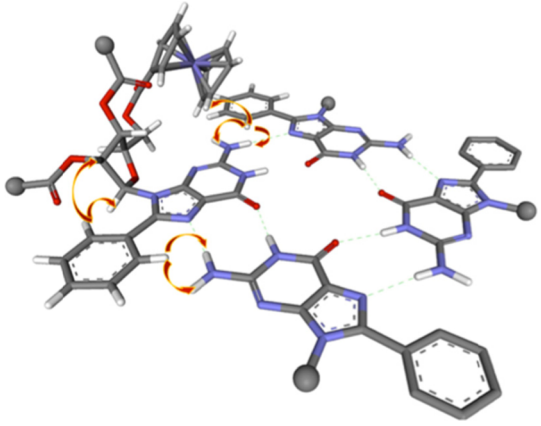

Figure 2. Proposed model for the isolated G_4 formed by **8Ph5Fc**. Arrows indicate selected NOEs. Some atoms are omitted for clarity.

Stabilization of this structure by residual water[27] seems unlikely because in no case did we observe in NOE spectra a signal in the 1.5−2.5 ppm region, except for the expected exchange signals with N(1)H and N(2)H.

To gain deeper insights into the propensity of the derivatives to undergo self-assembly, we have extended our study to atomic force microscopy (AFM) imaging. In addition to **8Ph5Fc**, derivatives **8Fc5C10** and **8Ph5C10** were studied for comparison. The samples were prepared by drop-casting 150 μL of guanosine solutions in CH_2Cl_2 (concentration 0.6 mg/mL) onto the basal plane of thermally grown SiO_2/Si (230 nm SiO_2 on Si [100]). Prior use, the substrates were cleaned and functionalized with a monolayer of hexamethyldisilazane (HMDS), covalently bonded to the pending SiOH groups, in order to render the surface hydrophobic and to avoid the formation of hydrogen bonds between the molecules and the substrate. Figure 3 displays the topographical AFM images of films of **8Ph5Fc** (Figure 3a,c) and **8Fc5C10** (Figure 3b,d) prepared using the same experimental conditions.

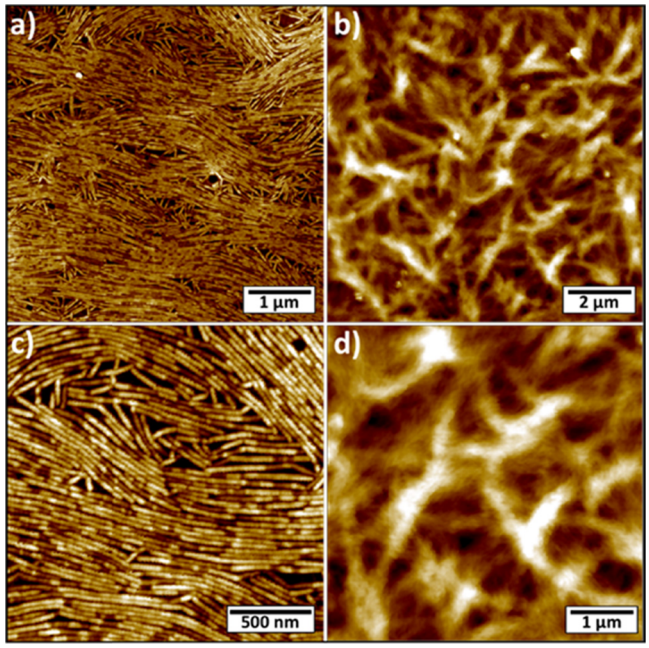

Figure 3. AFM images of supramolecular metal-free G aggregates drop-cast from CH_2Cl_2 0.6 mg/mL on HMDS-functionalized SiO_2. (a,c) Molecule **8Ph5Fc**. (b,d) Molecule **8Fc5C10**. Images Z-scales: (a) 10 nm; (b) 140 nm; (c) 7 nm; and (d) 110 nm.

The observed morphologies are markedly different. Molecule **8Fc5C10** forms a disordered network of entangled bundles of fibers, while **8Ph5Fc** self-assembles into layers of ordered and well-aligned fibers possessing an average height of 4.1 ± 0.5 nm (measured with respect to the widest empty areas) and an average width of 32 ± 4 nm. Being the lateral size of the fibers comparable to the curvature radius of the used AFM tips (nominal radius 7 nm), the measured width value must be corrected to exclude the broadening artifact given by the mechanical convolution effect. Considering the measured width and an interfiber penetration of the tip of ∼1.8 nm, we can apply well-established models[28] to conclude that the real width of such fibers amounts to 19 ± 4 nm. As the radius of the G-quartet structure in columnar aggregates, both in water[29] and in organic solvents,[17] amounts to 12.5 Å and a fully elongated decanoyl residue measures ca.12 Å, it is possible to estimate a diameter of 4.8 nm for the G_4*s* formed by **8Ph5Fc**. This value is in good agreement with the average measured height for the fibers. Assuming a 3.3 Å spacing (characteristic of optimal nucleobase stacking[30]), the cylindrical fibers shown in Figure 3a,c are composed on an average of six stacked G_4s.

To promote the aggregation into more stable and ordered supramolecular structures, the films were then exposed to solvent vapor annealing (SVA) in CH_2Cl_2 for 48 h under ambient conditions. Such a method makes it possible to trigger the molecular reorganization toward the generation of thermodynamically favored architectures. It is noteworthy that this method has previously been successfully used to finely tune the self-assembly of various molecular systems, including *n*-type perylene nanowires,[31] p-type pentacene,[32] hexa-*peri*-hexabenzocoronene (HBC)[33] structures, and porphyrins.[34] Figure 4 portrays the AFM images of the **8Ph5Fc** (a,c) and

https://doi.org/10.1021/acs.joc.1c00502
J. Org. Chem. 2021, 86, 9970−9978

8Fc5C10 (b,d) fibers formed on the surface after the SVA treatment.

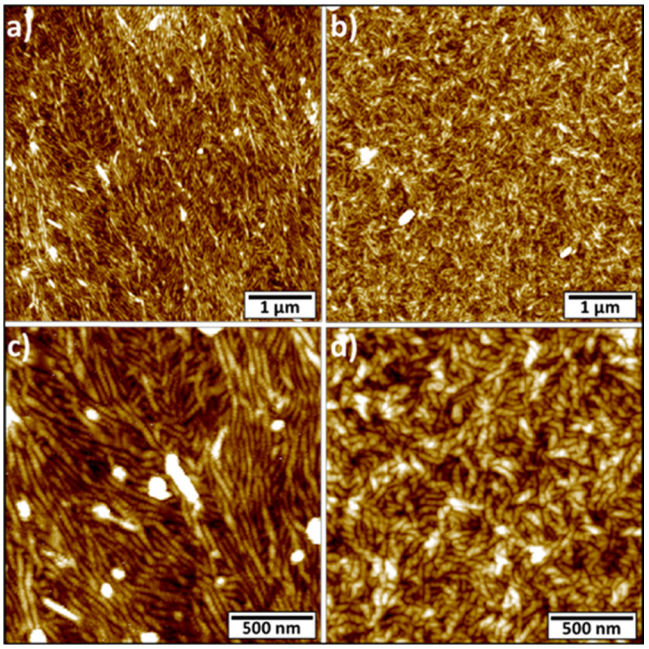

Figure 4. AFM images of supramolecular metal-free G aggregates drop-cast from CH_2Cl_2 0.6 mg/mL on HMDS-functionalized SiO_2 after SVA (CH_2Cl_2 for 48 h). (a,c) Compound **8Ph5Fc**. (b,d) Compound **8Fc5C10**. Images Z-scales: (a) 13 nm; (b) 25 nm; (c) 12 nm; and (d) 20 nm.

Interestingly, the two compounds showed a similar behavior: in both cases, SVA caused an increased entanglement of the fibrillar structures, resulting in an extremely uniform coverage of the underneath substrate, which is no longer exposed. In particular, in the case of **8Ph5Fc**, the as-deposited fibers show high rigidity and no tendency to entangle, causing the formation of holes and discontinuities in the resulting films, as shown in Figure 3a,c. After the SVA treatment, the fibers assemble into less-ordered bundles, forming a multilayered uniform film (Figure 4a,c). In the latter case, the fibers feature an average measured width of 41 ± 3 nm, suggesting that the packing at the molecular level is not affected by the SVA treatment, but it is not possible to correct the data with the previously used model because of the multilayer nature of the film after SVA. In the case of compound **8Fc5C10**, the SVA process exhibits a strong impact over the morphology of the films that undergo a dramatic decrease in roughness from 23.2 nm (before SVA, Figures 3b,d) to 4.15 nm (after SVA, Figures 4b,d). Moreover, the compound **8Fc5C10** fibers show completely different conformations: before SVA, the fibrillar structure is hardly visible, while after that, the fibrillar units are extremely well defined and form a strongly entangled network.

On the other hand, samples of **8Ph5C10** showed no tendency to form crystalline structures. In this case, AFM characterization has not revealed any well-defined structures, and the films look amorphous (see Figure S18).

CONCLUSIONS

In summary, we have designed and synthesized several organic soluble guanosines carrying either a phenyl or a ferrocenyl group at the C(8) position. Their self-assembly has been studied in solution by NMR and in thin films by means of AFM. Derivative **8Ph5Fc** shows the exclusive existence of isolated G_4s in the CD_2Cl_2 solution, while compounds **8Fc5C10** and **8Ph5C10** do form isolated G_4s as well, but another aggregated species is present in equilibrium in solution. The hierarchical self-assembly of **8Ph5Fc** and **8Fc5C10** leads to the formation of fibers, which can be deposited and characterized on surfaces. Guanosine **8Fc5C10** shows the formation of a disordered film, arising from the coexistence of different self-assembled species (probably a mixture of stacked G_4s and H-bonded dimeric/oligomeric ribbon-like aggregates), whereas **8Ph5Fc** cleanly assembles into unprecedented, stacked cation-free G_4 architectures. The ferrocenyl moiety of **8Fc5C10** seems to be not large enough to drive the self-assembly toward the exclusive existence of isolated G_4s in solution, while its shape seems to hamper π-stacking and hence a shift in equilibria toward (stacked) quartets in the solid state. On the other hand, the results obtained for **8Ph5C10** indicate that the self-assembly is not ruled uniquely by the nature of the C(8) substituent: the behavior observed only for **8Ph5Fc** suggests that also the nature of the 5′ substituent, although irrelevant for G_4 formation, affects the subsequent self-assembly. These results further expand the range of supramolecular architectures that can be obtained in thin films and provide unambiguous evidence for the key role played by the subtle design of guanosine starting building blocks to control the hierarchical self-assembly motifs that can be attained.

EXPERIMENTAL PROCEDURES

General Methods. All reactions that require anhydrous conditions were carried out under a dry argon atmosphere in oven-dried glassware. Macherey-Nagel polygram silica gel plates (layer thickness 0.20 mm) were used for thin layer chromatography (TLC) analyses. Column chromatography was performed on Geduran silica gel 60 (40−63 μm). Reagents and solvents, including dry solvents, were purchased from Sigma-Aldrich or TCI. Electrospray ionization (ESI) mass spectra were obtained from methanol solutions in either the positive or negative mode, with Micromass ZMD 4000 or ZQ-4000 instruments. High-resolution mass spectrometry (HRMS) spectra were recorded on a Waters Xevo G2-XS QTof system. Nuclear magnetic resonance (NMR) spectra were recorded on Varian Inova (600, 400, or 300 MHz) spectrometers and referenced to the residual solvent resonance (s = singlet, bs = broad singlet, d = doublet, t = triplet, q = quartet, qi = quintet, m = multiplet; coupling constant are in Hz). Structural assignments were made with additional information from gCOSY (gradient-selected correlation spectroscopy), gHSQC (gradient-selected heteronuclear single-quantum correlation), and gHMBC (gradient-selected heteronuclear multiple bond correlation) experiments. Diastereotopic protons/carbons were not assigned. CD spectra were recorded on a Jasco J-710 spectropolarimeter. Synthetic schemes with compound numbering are reported in the Supporting Information (S1−S4)

Microscopy Studies. The AFM study of the self-assembled **1**, **4**, and **5** was performed using Veeco/Bruker Dimension 3100 that runs with a Nanoscope IV controller. Solutions of investigated molecules were prepared in 0.6 mg/mL CH_2Cl_2 and deposited by drop-casting (150 μL) on clean SiO_2/Si (230 ± 10 nm SiO_2 on [100] Si) functionalized with a monolayer of HMDS. The SVA treatment was performed by placing the compound films in a sealed environment and saturating with CH_2Cl_2 vapor under ambient conditions, for 48 h. The raw AFM data were processed through the application of background flattening.

8-Bromo Guanosine ***9***. The compound was prepared according to a literature procedure.[35] Thus, commercial guanosine **5** (1.00 g, 3.53 mmol) was suspended in 60 mL of an acetonitrile/water 2:1 mixture,

https://doi.org/10.1021/acs.joc.1c00502
J. Org. Chem. 2021, 86, 9970−9978

and *N*-bromosuccinimide (943 mg, 5.3 mmol, 1.5 eq) was added in three portions over 20 min. Stirring was continued until TLC (CH_2Cl_2/MeOH 8:2) revealed the disappearance of the starting material (2 h). Solvents were then removed in vacuo, and the pale-yellow solid thus obtained was suspended in acetone (20 mL) and stirred at room temperature for 2 h. The flask was then placed in a refrigerator and left overnight at −20 °C. The precipitate was filtered and washed several times with cold acetone to afford 1.09 g, 3.02 mmol (yield 86%) of 8-bromo guanosine **9** as a white solid.

ESI-MS (*m*/*z*): 362.1/363.9 $[M + H]^+$; 383.9/386.0 $[M + Na]^+$; 360.1/362.0 $[M - H]^-$.

HRMS (ESI/Q-TOF) *m*/*z*: $[M + Na]^+$ calcd for $C_{10}H_{12}BrN_5O_5Na$ 383.9914; found 383.9919.

^{1}H-NMR (dmso-d_6, 600 MHz): δ 10.81 (bs, 1H, NH), 6.50 (bs, 2H, NH_2), 5.68 (d, 1H, *J* = 6.0 Hz, H1'), 5.44 (d, 1H, *J* = 6.0 Hz, OH2'), 5.08 (d, 1H, *J* = 5.1 Hz, OH3'), 5.01 (m, 1H, H2'), 4.92 (m, 1H, OH5'), 4.13 (m, 1H, H3'), 3.85 (m, 1H, H4'), 3.63 (m, 1H, H5'), 3.54 (m, 1H, H5'). $^{13}C\{^1H\}$ NMR (dmso-d_6, 75 MHz): δ 155.9, 153.9, 152.5, 121.5, 118.0, 90.1, 86.3, 70.9, 70.7, 62.5

8-Bromo-5′-O-tert-butyldimethylsilyl Guanosine ***10***. 8-Bromo guanosine **9** (1.274 g, 3.52 mmol) was dried at 50 °C over P_2O_5 in vacuo for 2 h and dissolved in dimethylformaimde (DMF) (17 mL). Imidazole (491 mg, 7.21 mmol, 2.05 eq) was added. To the resulting mixture was then added dropwise a solution of *t*-butyldimethylsilyl chloride (558 mg, 3.70 mmol, 1.05 eq.) in tetrahydrofuran (THF) (9 mL), and stirring was continued for 2 h. As TLC (CH_2Cl_2/MeOH 8:2) revealed the presence of unreacted starting material, an extra amount of imidazole (120 mg, 1.76 mmol, 0.5 eq.) and *t*-butyldimethylsilyl chloride (266 mg, 1.76 mmol, 0.5 eq.) was added, and reaction was continued for 2 h. The crude mixture was poured into water (50 mL), and the precipitate was filtered, washed with water and Et_2O, and dried to afford the product (1.04 g, 2.19 mmol, 62%) as a white solid.

RF = 0.6 (CH_2Cl_2/MeOH 8:2).

ESI-MS (*m*/*z*): 473.9/475.9 $[M - H]^-$; 475.9/477.9 $[M + H]^+$.

HRMS (ESI/Q-TOF) *m*/*z*: $[M + H]^+$ calcd for $C_{16}H_{27}BrN_5O_5Si$ 476.0959; found 476.0965.

^{1}H-NMR (CD_3OD, 600 MHz): δ 5.85 (d, 1H, *J* = 4.2 Hz, H1'), 5.26 (dd, 1H, *J* = 5.7 Hz, *J* = 4.2 Hz, H2'), 4.56 (m, 1H, *J* = 5.7 Hz, H3'), 3.95 (m, 1H, *J* = 11.4 Hz, *J* = 5.7 Hz, *J* = 4.0 Hz, H4'), 3.92 (1H, dd, *J* = 11.4 Hz, *J* = 4.0 Hz, H5'), 3.83 (dd, 1H, *J* = 11.4 Hz, *J* = 5.7 Hz, H5'), 0.84 (s, 9H, *t*BuSi), 0.01 and −0.03 (s,s, 6H, $SiMe_2$). $^{13}C\{^1H\}$ NMR (CD_3OD, 151 MHz): δ

8-Phenyl-5′-O-tert-butyldimethylsilyl Guanosine ***11***. $PdCl_2(PPh_3)_2$ (59.0 mg, 0.084 mmol, 0.2 eq.) was added to a degassed solution of **10** (200 mg, 0.421 mmol), phenylboronic acid (77 mg, 0.630 mmol, 1.5 eq.), and K_3PO_4 (223 mg, 1.05 mmol) in 7 mL of a 6:1 mixture of dioxane/water. The mixture was heated at 95 °C for 22 h in an oil bath. After cooling to room temperature, solvents were removed by distillation, the dark residue was suspended in 50 mL of Et_2O and filtered. The filtrate was washed with brine (40 mL) and 1 N HCl (6 mL) and then dried over $MgSO_4$. The precipitate was washed with a CH_2Cl_2/MeOH 4:1 mixture; washings were combined with the ethereal residue, and solvents were removed in vacuo. The residue was purified by column chromatography on silica gel (CH_2Cl_2/MeOH 95:5), and the product was obtained in a 61% yield (121 mg, 0.256 mmol) as a white solid.

RF = 0.2 (CH_2Cl_2/MeOH 9:1).

ESI-MS (*m*/*z*): 472.4 $[M - H]^-$; 474.1 $[M + H]^+$; 496.2 $[M + Na]^+$.

HRMS (ESI/Q-TOF) *m*/*z*: $[M + H]^+$ calcd for $C_{22}H_{32}N_5O_5Si$ 474.2167; found 474.2173.

^{1}H-NMR (dmso-d_6, 600 MHz): δ 10.73 (bs, 1H, NH), 7.67−7.64 (m, 2H, ArH), 7.54−7.52 (m, 3H, ArH), 6.43 (bs, 2H, NH_2), 5.60 (d, 1H, *J* = 5.5 Hz, H1'), 5.36 (d, 1H, *J* = 6.0 Hz, OH), 5.07 (m, 1H), 4.94 (d, 1H, *J* = 6.0 Hz, OH), 4.13 (m, 1H), 3.84−3.74 (m, 3H, H4',H5', H5″), 0.841 (s, 9H, *t*BuSi), 0.006 and 0.003 (s,s, 6H, $SiMe_2$). $^{13}C\{^1H\}$ NMR (dmso-d_6, 75 MHz): δ 157.2 (C), 153.5 (C), 152.7 (C), 147.8 (C), 130.7 (C), 129.9 (CH, Ph), 129.5 (CH, Ph), 129.1 (CH, Ph), 117.4 (C), 89.7 (C1'), 85.3 (C4'), 70.7 (C3'), 70.5 (C2'), 64.1 (C5'), 26.3 (CH_3), 18.5 (C), −4.8 (CH_3), −4.8 (CH_3).

8-Phenyl-5′-O-tert-butyldimethylsilyl-2′,3′-O-didecanoyl Guanosine ***3*** *(8Ph5Si)*. 8-Phenyl-5′-O-*tert*-butyldimethylsilyl guanosine **11** (100 mg, 0.211 mmol) was dried in vacuo over P_2O_5 at 50 °C for 1 h and dissolved in 15 mL of an acetonitrile/toluene 2:1 mixture. Decanoic anhydride (163 μL, 0.444 mmol, 2.10 eq.), Et_3N (64 μL, 0.444 mmol, 2.10 eq.), and a small amount of 4-dimethylaminopyridine (DMAP) were then added, and the mixture was heated at 80 °C in an oil bath for 7 h. After cooling to room temperature, MeOH (0.5 mL) was added, and stirring was continued for 20 min. Solvents were removed by distillation, the residue was dissolved in CH_2Cl_2, washed with 5% $NaHCO_3$ and brine, and dried over $MgSO_4$. After the removal of solvents, the residue was purified by chromatography on silica gel (CH_2Cl_2/MeOH 99:1), and the product (120 mg, 0.153 mmol) was obtained as a white solid in 72% yield.

RF = 0.36 (CH_2Cl_2/MeOH 97:3).

ESI-MS (*m*/*z*): 780.6 $[M - H]^-$; 782.6 $[M + H]^+$; 804.6 $[M + Na]^+$.

HRMS (ESI/Q-TOF) *m*/*z*: $[M + Na]^+$ calcd for $C_{42}H_{67}N_5O_7SiNa$ 804.4702; found 804.4713.

^{1}H-NMR (CD_2Cl_2, 600 MHz): δ 12.38 (bs, 1H, NH), 7.77 (d, 2H, *orto*-ArH), 7.54−7.59 (m, 3H, ArH), 6.37 (m, 1H, H2'), 6.17 (m, 1H, H3'), 5.77 (d, 1H, *J* = 3.2 Hz, H1'), 4.14 (m, 1H, H4'), 3.90 (1H, dd, *J* = 12.0 Hz, 4.2 Hz, H5'), 3.78 (dd, 1H, *J* = 12.0 Hz, 5.0 Hz, H5'), 2.28 (t, 2H, $-CH_2-CO$), 2.24 (t, 2H, $-CH_2-CO$), 1.60 (m, 2H, CH_2-CH_2-CO), 1.52 (m, 2H, CH_2-CH_2-CO), 1.28−1.23 (m, 24H, CH_2), 0.87 and 0.85 (t,t, 6H, CH_3), 0.78 (s, 9H, *t*BuSi), 0.07 and 0.04 (s,s, 6H, $SiMe_2$). $^{13}C\{^1H\}$ NMR (CD_2Cl_2, 151 MHz): δ 172.4 (C═O), 172.3 (C═O), 159.4 (C), 153.6 (C), 152.4 (C4), 148.6 (C8), 130.0 (CH, Ph), 129.5 (C), 129.3 (CH, Ph), 129.1 (CH, Ph), 116.9 (C), 87.5 (C1'), 82.0 (C4'), 72.1 (C2'), 70.3 (C3'), 62.6 (C5'), 34.0 (CH_2), 33.9 (CH_2), 32.01 (CH_2), 31.97 (CH_2), 29.6 (CH_2), 29.5 (CH_2), 29.5 (CH_2), 29.4 (CH_2), 29.4 (CH_2), 29.2 (CH_2), 29.1 (CH_2), 25.6 (CH_3), 24.9 (CH_3), 24.9 (CH_2), 22.8 (CH_2), 22.8 (CH_2), 18.2 (C), 14.0 (CH_3), 14.0 (CH_3), −5.6 (CH_3), −5.7 (CH_3).

8-Phenyl-2′,3′-O-didecanoyl Guanosine ***2*** *(8Ph5OH)*. To a solution of **3** (120 mg, 0.153 mmol) in THF (4 mL) were added 72.5 mg (0.230 mmol, 1.5 eq) of tetra-*n*-butylammonium fluoride (TBAF). The mixture was stirred at room temperature until TLC (CH_2Cl_2/MeOH 92:8) showed complete disappearance of the starting material. The reaction mixture was concentrated, redissolved in CH_2Cl_2, and washed with sat. $NaHCO_3$ (3 × 10 mL). The organic phase was dried over $MgSO_4$, and solvents were removed by distillation. The residue was purified on silica gel by first eluting with Et_2O and then with CH_2Cl_2/MeOH 95:5. The product was obtained as a white solid in a 73% yield (75 mg, 0.112 mmol).

RF = 0.28 (CH_2Cl_2/MeOH 92:8).

ESI-MS (*m*/*z*): 666.6 $[M - H]^-$; 668.4 $[M + H]^+$; 690.4 $[M + Na]^+$.

HRMS (ESI/Q-TOF) m/z: $[M + Na]^+$ calcd for $C_{36}H_{53}N_5O_7Na$ 690.3837; found 690.3846.

^{1}H-NMR (dmso-d_6, 600 MHz): δ 10.84 (bs, 1H, NH), 7.61−7.58 (m, 2H, *o*-ArH), 7.55−7.53 (m, 3H, *m*- and *p*-ArH), 6.48 (bs, 2H, NH_2), 6.18 (t, 1H, OH), 5.78 (d, 1H, *J* = 6.0 Hz, 1'H), 5.49 (m, 1H, 2'H), 5.18 (m, 1H, 3'H), 4.08 (m, 1H, 4'H), 3.75 (m, 1H, 5'H), 3.64 (m, 1H, 5'H), 2.35−2.16 (m, 4H, CH_2-CO), 1.48 and 1.40 (qi, qi, 4H, CH_2-CH_2-CO), 1.27−1.12 (m, 24H, CH_2), 0.85 and 0.84 (t,t, 6H, CH_3). $^{13}C\{^1H\}$ NMR (dmso-d_6, 151 MHz): δ 172.3 (C═O 3′), 171.8 (C═O 2′), 159.6 (C), 153.7 (C), 153.5 (C), 147.4 (C8), 131.9 (CH, *p*-Ph), 130.5 (C, Ph), 129.9 (CH, *o*-Ph), 129.2 (CH, *m*-Ph), 119.6 (C), 88.1 (C1'), 85.1 (C4'), 72.1 (C3'), 71.7 (C2'), 61.6 (C5'), 33.9 (CH_2), 33.6 (CH_2), 31.8 (CH_2), 29.3 (CH_2), 29.3 (CH_2), 29.3 (CH_2), 29.2 (CH_2), 29.2 (CH_2), 29.2 (CH_2), 29.0 (CH_2), 28.9 (CH_2), 24.8 (CH_2), 24.5 (CH_2), 22.6 (CH_2), 14.0 (CH_3).

8-Phenyl-5′-O-ferrocenoyl-2′,3′-O-didecanoyl Guanosine ***1*** *(8Ph5Fc)*. Ferrocene carboxylic acid (77.5 mg, 0.337 mmol, 1.3 eq.) was dried in vacuo at 50 °C for 1 h and dissolved in THF (9 mL). Et_3N (175 μL, 1.217 mmol, 4.7 eq.) was added, and the resulting

https://doi.org/10.1021/acs.joc.1c00502
J. Org. Chem. 2021, 86, 9970−9978

solution was cooled to 0 °C. Methanesulfonyl chloride (25.5 μL, 0.311 mmol, 1.2 eq.) was added, and the mixture was allowed to warm to room temperature and stirred for 2 h. A solution of vacuum-dried 8-phenyl-2′,3′-O-didecanoyl guanosine **2** (173 mg, 0.259 mmol) in THF (6 mL) was then added, followed by a catalytic amount of DMAP. Stirring was continued for 24 h, MeOH (0.5 mL) was added, and the reaction mixture was concentrated in vacuo. The residue was dissolved in CH_2Cl_2, washed with water, and dried over $MgSO_4$. The solvent was removed by distillation, and the residue was purified by chromatography on silica gel (gradient from CH_2Cl_2 to CH_2Cl_2/MeOH 99:1), affording the product (85 mg, 0.097 mmol) as a yellow solid in 38% yield.

RF = 0.24 (CH_2Cl_2/MeOH 9:1).

ESI-MS (*m*/*z*): 878.6 $[M - H]^-$; 880.5 $[M + H]^+$; 902.5 $[M + Na]^+$.

HRMS (ESI/Q-TOF) *m*/*z*: $[M + Na]^+$ calcd for $C_{47}H_{61}FeN_5O_8Na$ 902.3762; found 902.3776.

^{1}H-NMR (CD_2Cl_2, 600 MHz): δ 12.57 (bs, 1H, NH), 7.81 (d, 2H, *J* = 7.1 Hz, Ph), 7.56 (t, 2H, *J* = 7.1 Hz, Ph), 7.49 (t, 1H, *J* = 7.1 Hz, Ph), 6.48 (dd, 1H, *J* = 7.8 Hz, 5.4 Hz, H3′), 6.43 (dd, 1H, *J* = 5.4 Hz, 3.0 Hz, H2′), 5.85 (d, 1H, *J* = 3.0 Hz, H1′), 4.67 (s, 1H, Fc), 4.62 (dd, 1H, *J* = 12.0 Hz, 4.3 Hz, H5′), 4.61 (s, 1H, Fc), 4.41 (m, 1H, H4′), 4.34 (dd, 1H, *J* = 12.0 Hz, 4.3 Hz, H5′), 4.20 (s, 1H, Fc), 4.17 (s, 1H, Fc), 3.97 (s, 5H, Fc), 2.36−2.26 (m, 4H, C$\underline{H}_2$−CO), 1.67−1.52 (m, 4H, C$\underline{H}_2$−CH_2−CO), 1.33−1.20 (m, 24H, CH_2), 0.88−0.84 (m, 6H, CH_3). ^{13}C{^{1}H} NMR (CD_2Cl_2, 151 MHz): δ 172.5 (C, C$\underline{O}$(3′)), ′)), 117.1 (C), 87.6 (CH, C1′), 79.9 (CH, C4′), 72.5 (CH, C2′), 71.8 (CH, Fc), 71.7 (CH, Fc), 70.1 (C, Fc), 70.1 (CH, Fc), 70.0 (CH, C3′), 69.8 (CH, Fc), 61.7 (CH_2, C5′), 34.0 (CH_2), 33.9 (CH_2), 32.0 (CH_2), 32.0 (CH_2), 29.8 (CH_2), 29.6 (CH_2), 29.5 (CH_2), 29.5 (CH_2), 29.4 (CH_2), 29.4 (CH_2), 29.2 (CH_2), 29.1 (CH_2), 25.7 (CH_2), 24.9 (CH_2), 22.8 (CH_2), 14.0 (CH_3)

8-Phenylguanosine ***12***. To a degassed mixture of **9** (273 mg, 0.754 mmol), phenylboronic acid (110 mg, 0.902 mmol), Na_2CO_3 (160 mg, 1.51 mmol), tris(3-sulfonatophenyl)phosphine (TPPTS) (11 mg, 0.0194 mmol) in H_2O (2.4 mL), and acetonitrile (1.2 mL) were added 44 mg (0.0196 mmol) of $Pd(OAc)_2$, and the reaction mixture was stirred at 83 °C in an oil bath overnight. TLC (RP18, H_20/CH_3OH 1:1) confirmed the disappearance of the starting material. The reaction mixture was then cooled to room temperature and diluted with water (20 mL). The pH was adjusted to 7 with 1 N HCl. The resulting suspension was refluxed for a short time, cooled to room temperature, and maintained at 4 °C for 2 h. The precipitate was filtered, washed with water, and air-dried to afford the product as a white solid in 80% yield (216 mg, 0.60 mmol). The compound was sufficiently pure and was used in the following step without further purification.

ESI-MS (*m*/*z*): 360.2 $[M - H]^+$.

HRMS (ESI/Q-TOF) *m*/*z*: $[M + H]^+$ calcd for $C_{16}H_{18}N_5O_5$, 360.1302; found 360.1308.

^{1}H-NMR (dmso-d_6, 400 MHz): δ 10.75 (s, 1H, NH), 7.68−7.65 (m, 2H, Ph), 7.54−7.52 (m, 3H, Ph), 6.38 (bs, 2H, NH_2), 5.64 (d, 1H, *J* = 6.4 Hz, H1′), 5.36 (d, 1H, *J* = 6.4 Hz, $OH_{2'}$), 5.05−5.00 (m, 2H, H2′, $OH_{5'}$), 4.96 (d, 1H, *J* = 5.6 Hz, $OH_{3'}$), 4.09−4.06 (m, 1H, H3′), 3.85−3.81 (m, 1H, H4′), 3.70−3.65 (m, 1H, H5′), 3.58−3.52 (m, 1H, H5′).^{13}C{^{1}H} NMR (dmso-d_6, 101 MHz): δ 157.0 (C), 153.5 (C), 152.4 (C), 147.9 (C), 130.5 (C, Ph), 129.8 (CH, Ph), 129.6 (CH, Ph), 129.0 (CH, Ph), 117.6 (C), 89.4 (CH), 86.3 (CH), 71.0 (CH), 70.7 (CH), 62.5 (CH_2).

8-Phenyl-2′,3′,5′-O-tridecanoyl Guanosine ***4*** *(**8Ph5C10**)*. To a stirred suspension of **12** (97 mg, 0.27 mmol) in MeCN (4 mL) were added Et_3N (0.19 mL, 1.35 mmol), decanoic anhydride (0.33 mL, 0.89 mmol), and a catalytic amount of DMAP. The mixture was stirred at room temperature and monitored by TLC (DCM/MeOH 8:2). After 2 h, the mixture was concentrated under reduced pressure, and the resulting oil was partitioned between DCM and water. The organic layer was collected, the solvent was removed by distillation, and the residue was purified by column chromatography on silica (DCM/acetone 9:2.5 to remove decanoic acid and then DCM/MeOH 9:1) to afford triester **4** as a white waxy solid in 59% yield (131 mg, 0.16 mmol).

ESI-MS (*m*/*z*): 822.6 $[M + H]^+$, 844.6 $[M + Na]^+$.

HRMS (ESI/Q-TOF) *m*/*z*: $[M + Na]^+$ calcd for $C_{46}H_{71}N_5O_8Na$ 844.5195; found 844.5200.

^{1}H-NMR (CD_2Cl_2, 600 MHz): δ 12.43 (bs, 1H, NH), 7.74 (m, 2H, *o*-Ph), 7.58 (m, 2H, *m*-Ph), 7.53 (m, 1H, *p*-Ph), 6.29 (dd, 1H, *J* = 5.6 Hz, 3.8 Hz, H2′), 6.16 (t, 1H, *J* = 5.9 Hz, H3′), 5.86 (d, 1H, *J* = 3.7 Hz, H1′), 4.52 (m, 1H, H5′), 4.30 (m, 1H, H4′), 4.26 (m, 1H, H5′), 2.33−2.21 (m, 6H, CH_2−C$\underline{H}_2$−CO), 1.64−1.59 (m, 2H, C$\underline{H}_2$−CH_2−CO), 1.53−1.49 (m, 4H, 2 C$\underline{H}_2$−CH_2−CO), 1.31−1.18 (m, 36H, CH_2), 0.87 (t, 3H, CH_3), 0.85 (t, 3H, CH_3), 0.81 (t, 3H, CH_3).^{13}C{^{1}H} NMR (CD_2Cl_2, 151 MHz): δ 173.4 ($CO^{5'}$) 172.4 (CO), 172.2 (CO), 159.2 (C), 153.7 (C), 152.2 (C4), 148.3 (C8), 129.9 (Ph), 129.4 (Ph), 129.3 (Ph), 129.1 (Ph), 117.1 (C5), 87.7 (CH, C1′), 79.4 (CH, C4′), 72.3 (CH, C2′), 70.6 (CH, C3′), 62.8 (CH_2, C5′), 34.0 (CH_2), 34.0 (CH_2), 33.9 (CH_2), 32.0 (CH_2), 32.0 (CH_2), 31.9 (CH_2), 29.6 (CH_2), 29.5 (CH_2), 29.5 (CH_2), 29.4 (CH_2), 29.4 (CH_2), 29.4 (CH_2), 29.3 (CH_2), 29.2 (CH_2), 29.1 (CH_2), 24.9 (CH_2), 24.9 (CH_2), 24.9 (CH_2), 22.8 (CH_2), 22.8 (CH_2), 22.7 (CH_2), 14.0 (CH_2), 13.9 (CH_3).

8-Ferrocenylguanosine ***13***. A mixture of **9** (0.300 g, 0.83 mmol), dimethoxyethane (DME) (12 mL), ferroceneboronic acid (0.286 g, 1.24 mmol, 1.5 eq), and NaOH (3 M, 5.25 mL, 15.75 mmol) was degassed with a stream of Ar for 40 min in an ultrasonic bath. $PdCl_2(PPh_3)_2$ (0.058 g, 0.1 eq) was added, and the resulting solution was refluxed at 85 °C under argon in an oil bath for 48 h. The solvent was then removed under reduced pressure, the reaction mixture was neutralized with 10% HCl, and the solid was filtered, washed with water, and dried. The product thus obtained was used in the subsequent step without further purification.

An analytical sample was obtained by chromatography on silica (DCM/MeOH 8:2).

RF = 0.17 (DCM/MeOH 9:1).

ESI-MS (*m*/*z*): 466.3 $[M - H]$; 468.1 $[M + H]^+$; 490.1 $[M + Na]^+$.

HRMS (ESI/Q-TOF) *m*/*z*: $[M + Na]^+$ calcd for $C_{20}H_{21}FeN_5O_5Na$ 490.0784; found 490.0790.

^{1}H-NMR (dmso-d_6, 600 MHz): δ 10.67 (bs, 1H, NH), 6.65 (d, 1H, *J* = 7.2 Hz, H1′), 6.3 (bs, 2H, NH_2), 5.53 (d, 1H, *J* = 6.0 Hz, $OH^{2'}$), 5.36 (d, 1H, *J* = 6.0 Hz, $OH^{3'}$), 5.24 (m, 1H, $OH^{5'}$), 5.16 (m, 1H, H2′), 4.68 (s, 2H, Fc), 4.62 (s, 2H, Fc), 4.31 (s, 5H, Fc), 4.19 (m, 1H, H3′), 3.97 (m, 1H, H4′), 3.71 and 3.57 (m, m, 2H, H5′,H5).″^{13}C{^{1}H} NMR (dmso-d_6, 151 MHz): δ 157.8, 153.3, 152.4, 146.9, 117.7, 86.3, 80.4, 75.2, 71.8, 70.8, 70.2, 70.1, 69.9, 69.6, 68.9, 62.8.

8-Ferrocenyl-2′,3′,5′-O-tridecanoyl Guanosine ***5*** *(**8Fc5C10**)*. Crude 8-ferrocenylguanosine **13** (0.430 g, 1.0 eq, 0.92 mmol) was dried over P_2O_5 in vacuo for 2 h at 55 °C and then suspended in 30 mL of an acetonitrile−toluene 1:1 mixture. Decanoic anhydride (443 μL, 3.15 eq, 2.90 mmol) and triethylamine (209 μL, 3.15 eq, 2.90 mmol) were then added, followed by a catalytic amount of 4-dimethylamino pyridine. The mixture was stirred under argon for 14 h at 80 °C in an oil bath. A second aliquot of decanoic anhydride (443 μL, 3.15 eq, 2.90 mmol) and triethylamine (TEA) (209 μL, 3.15 eq, 2.90 mmol) was added, and stirring was continued for 12 h at the same temperature. The solvent was removed under reduced pressure, and the crude was dissolved in dichloromethane and extracted with a sat. $NaHCO_3$ and brine. The organic layer was dried over $MgSO_4$. The crude reaction mixture was then applied to a silica gel column packed in DCM and eluted with a mixture of DCM−methanol (from 99:1 to 95:5). The product was obtained as an orange glass in 23% yield (196 mg, 0.21 mmol).

ESI-MS (*m*/*z*): 930.5 $[M + H]^+$; 952.4 $[M + Na]^+$.

HRMS (ESI/Q-TOF) *m*/*z*: $[M + H]^+$ calcd for $C_{50}H_{76}FeN_5O_8$ 930.5038; found 930.5042.

^{1}H-NMR (dmso-d_6, 600 MHz): δ 10.77 (bs, 1H, NH), 6.75 (d, 1H, *J* = 6.0 Hz, H1′), 6.58 (t, 1H, *J* = 6.0 Hz, H2′), 6.40 (bs, 2H, NH_2), 5.74 (dd, 1H, *J* = 6.0 Hz, 4.2 Hz, H3′), 4.64 (s, 1H, Fc), 4.60 (s, 1H, Fc), 4.50 (bs, 2H, Fc), 4.48 (m, 1H, H5′), 4.37 (m, 1H, H4′),

https://doi.org/10.1021/acs.joc.1c00502
J. Org. Chem. 2021, 86, 9970−9978

4.30 (m, 1H, H5'), 4.28 (s, 5H, Fc), 2.45−2.27 (m, 6H, CH_2−C$\underline{H}_2$−CO), 1.58 (qi, 2H, J = 6.6 Hz, C$\underline{H}_2$−CH_2−CO), 1.47 (m, 4H, 2 C$\underline{H}_2$−CH_2−CO), 1.24−1.17 (m, 36H, CH_2), 0.85−0.82 (m, 9H, CH_3). $^{13}C\{^1H\}$ NMR (dmso-d_6, 151 MHz): δ 175.0 (CO), 173.1 ($CO^{5'}$), 172.2 ($CO^{2'}$), 156.6 (C), 153.6 (C), 152.6 (C4), 146.1 (C8), 117.3 (C5), 86.6 (CH, C1'), 80.1 (CH, C4'), 74.5 (C, Fc), 71.1 (CH, C3'), 70.6 (CH, C2'), 70.2 (CH, Fc), 70.0 (CH, Fc), 69.8 (CH, Fc), 68.7 (CH, Fc), 68.6 (CH, Fc), 63.0 (CH_2, C5'), 34.1 (CH_2), 33.9 (CH_2), 33.8 (CH_2), 33.6 (CH_2), 31.7 (CH_2), 29.3 (CH_2), 29.3 (CH_2), 29.2 (CH_2), 29.2 (CH_2), 29.1 (CH_2), 29.1 (CH_2), 29.0 (CH_2), 29.0 (CH_2), 28.8 (CH_2), 28.8 (CH_2), 25.0 (CH_2), 24.9 (CH_2), 24.8 (CH_2), 24.7 (CH_2), 22.5 (CH_2), 14.4 (CH_3), 14.4 (CH_3).

8-Ferrocenyl-5′-O-tert-butyldimethylsilyl Guanosine ***14***. A mixture of **13** (0.135 g, 0.29 mmol), imidazole (39 mg, 0.58 mmol), and *t*-butyldimethylsilyl chloride (48 mg, 0.32 mmol) in DMF (3 mL) was stirred at room temperature for 2 h. After the completion of the reaction (TLC DCM/MeOH 8:2), water (10 mL) was added, and the resulting precipitate was filtered and washed with water. The dry residue was purified by column chromatography (DCM/MeOH 92:8) to afford the product as a white solid in 62% yield (104 mg, 0.18 mmol).

RF = 0.6 (CH_2Cl_2/MeOH 8:2).

ESI-MS (m/z): 580.4 $[M - H]^-$; 582.1 $[M + H]^+$; 604.2 $[M + Na]^+$.

HRMS (ESI/Q-TOF) m/z: $[M + H]^+$ calcd for $C_{26}H_{36}FeN_5O_5Si$ 582.1830; found 582.1835.

^{1}H-NMR (dmso-d_6, 400 MHz): δ 10.64 (s, 1H, NH), 6.51 (d, 1H, J = 5.6 Hz, H1'), 6.34 (bs, 2H, NH_2), 5.50 (d, 1H, J = 5.6 Hz, $OH_{2'}$), 5.27−5.23 (m, 1H, H2'), 5.07 (d, 1H, J = 5.6 Hz, $OH_{3'}$), 4.67−4.66 (m, 2H, Fc), 4.47−4.45 (m, 2H, Fc), 4.29 (s, 5H, Fc), 4.27 (m, 1H, H3'), 3.92−3.85 (m, 2H, H5', H4'), 3.79−3.75 (m, 1H, H5'), 0.82 (s, 9H, *t*BuSi), −0.014 and −0.010 (s,s, 6H, $SiMe_2$). $^{13}C\{^1H\}$ NMR (dmso-d_6, 101 MHz): δ 156.7, 153.1, 152.8, 146.7, 117.4, 89.3, 85.1, 75.2, 71.0, 70.4, 69.9, 69.9, 69.7, 69.2, 68.8, 64.2, 26.2, 18.4, −4.7, −4.8.

8-Ferrocenyl-5′-O-tert-butyldimethylsilyl-2′,3′-O-didecanoyl Guanosine ***6*** *(8Fc5Si)*. To a suspension of **14** (71 mg, 0.12 mmol) in MeCN (4 mL) were added Et_3N (45 μL, 0.32 mmol), decanoic anhydride (100 μL, 0.27 mmol), and a catalytic amount of DMAP. The mixture was stirred at room temperature for 4 h. MeOH (0.2 mL) was then added, and solvents were removed under reduced pressure. The residue was partitioned between DCM (20 mL) and water (10 mL). The organic layer was further washed with water (10 mL) and concentrated in vacuo to give an orange glassy solid, which was purified by column chromatography on silica (gradient from pure DCM to DCM/MeOH 97:3). Pure DCM (300 mL ca.) was used to elute decanoic acid, and then, DCM/MeOH 97:3 was used to elute two orange bands: the first one consisting of pure **6** (55 mg, 0.06 mmol, yield 50%), while the second one containing the desilylated derivative **7** formed during work-up.

ESI-MS (m/z): 888.7 $[M - H]^-$; 890.5 $[M + H]^+$, 912.6 $[M + Na]^+$.

HRMS (ESI/Q-TOF) m/z: $[M + H]^+$ calcd for $C_{46}H_{72}FeN_5O_7Si$ 890.4545; found 890.4533.

^{1}H-NMR (CD_2Cl_2, 600 MHz): δ 12.33 (bs, 1H, NH), 6.82 (d, 1H, J = 4.7 Hz, H1'), 6.74 (m, 1H, H2'), 6.18 (m,1H, H3'), 4.82 (bs, 2H, Fc), 4.53 (bs, 1H, Fc), 4.48 (bs, 1H, Fc), 4.27 (s, 5H, Fc), 4.28−4.24 (m, 1H, H4'), 3.94 (dd, 1H, J = 11.4 Hz, 4.7 Hz, H5'), 3.83 (dd, 1H, J = 11.4 Hz, 4.7 Hz, H5'), 2.38 (m, 2H, CH_2−C$\underline{H}_2$−CO), 2.33 (t, 2H, CH_2−C$\underline{H}_2$−CO), 1.70−1.64 (m, 2H, C$\underline{H}_2$−CH_2−CO), 1.61−1.56 (m, 2H, C$\underline{H}_2$−CH_2−CO), 1.36−1.23 (m, 24H, CH_2), 0.87 (t, 3H, CH_3), 0.84 (t, 3H, CH_3), 0.82 (s, 9H, t-Bu), 0.00 (s, 3H, SiMe), −0.030 (s, 3H, SiMe). $^{13}C\{^1H\}$ NMR (CD_2Cl_2, 151 MHz): δ 172.5 (CO), 172.2 (CO), 158.8 (C), 153.2 (C), 152.8 (C4), 148.2 (C8), 116.9 (C), 86.4 (CH, C1'), 82.4 (CH, C4'), 73.8 (C, Fc), 71.4 (CH, C2'), 70.7 (CH, C3'), 70.5 (CH, Fc), 70.2 (CH, Fc), 69.8 (CH, Fc), 69.0 (CH, Fc), 68.3 (CH, Fc), 62.6 (CH_2, C5'), 34.2 (CH_2), 34.0 (CH_2), 32.0 (CH_2), 31.9 (CH_2), 29.6 (CH_2), 29.5 (CH_2), 29.4 (CH_2), 29.4 (CH_2), 29.3 (CH_2), 29.2 (CH_2), 25.6 (CH_3), 25.1 (CH_2), 24.9 (CH_2), 22.8 (CH_2), 22.7 (CH_2), 18.2 (C), 14.0 (CH_3), −5.6 (SiMe).

8-Ferrocenyl-2′,3′-O-didecanoyl Guanosine ***7*** *(8Fc5OH)*. To a solution of **6** (55 mg, 0.06 mmol) in 3 mL of THF were added 30 mg (0.09 mmol) of TBAF·$3H_2O$, and the mixture was stirred at room temperature for 20 h. The solvent was removed by evaporation, and the residue was dissolved in DCM (15 mL) and washed sequentially with 5% $NaHCO_3$ (5 mL) and water (5 mL, 4 times). The organic fraction was then dried over Na_2SO_4, and the solvent was removed by distillation. The residue was purified by chromatography on silica gel (gradient from pure DCM to DCM/MeOH 96:4) to afford **7** (33 mg, 0.04 mmol) as yellowish glass in 69% yield.

RF = 0.32 (DCM/MeOH 95:5).

ESI-MS (m/z): 774.5 $[M - H]^-$; 776.3 $[M + H]^+$, 798.3 $[M + Na]^+$.

HRMS (ESI/Q-TOF) m/z: $[M + Na]^+$ calcd for $C_{40}H_{57}FeN_5O_7Na$ 798.3500; found 798.3506.

^{1}H-NMR (CD_2Cl_2, 600 MHz): δ 12.31 (bs, 1H, NH), 7.22 (d, 1H, J = 13.8 Hz, H1'), 6.98 (bs, 2H, NH_2), 6.50 (bs, 1H, OH), 6.12 (dd, 1H, J = 13.8 Hz, 7.2 Hz, H2'), 5.71 (d, 1H, J = 7.2 Hz, H3'), 4.78 (bs, 1H, Fc), 4.57 (bs, 2H, Fc), 4.52 (bs, 1H, Fc), 4.35 (s, 5H, Fc), 4.37−4.31 (m, 1H, H4'), 4.01−3.96 (m, 1H, H5'), 3.87−3.80 (m, 1H, H5'), 2.47 (t, 2H, CH_2−CO), 2.28 (t, 2H, CH_2−CO), 1.72 (m, 2H, C$\underline{H}_2$−CH_2−CO), 1.54 (m, 2H, C$\underline{H}_2$−CH_2−CO), 1.40−1.20 (m, 24H, CH_2), 0.88 (t, 3H, CH_3), 0.82 (t, 3H, CH_3). $^{13}C\{^1H\}$ NMR (CD_2Cl_2, 151 MHz): δ 172.5 (CO), 171.9 (CO), 158.5 (C), 153.5 (C), 151.7 (C), 148.1 (C), 117.5 (C), 86.2 (CH, C1'), 85.7 (CH, C4'), 73.6 (C, Fc), 72.9 (CH, C3'), 71.6 (CH, C2'), 70.9 (CH, Fc), 70.2 (CH, Fc), 69.7 (CH, Fc), 69.5 (CH, Fc), 68.8 (CH, Fc), 63.1 (CH_2, C5'), 34.5 (CH_2), 33.8 (CH_2), 32.0 (CH_2), 31.9 (CH_2), 29.6 (CH_2), 29.5 (CH_2), 29.4 (CH_2), 29.3 (CH_2), 29.1 (CH_2), 25.2 (CH_2), 24.7 (CH_2), 22.8 (CH_2), 14.0 (CH_3).

8-Ferrocenyl-5′-O-benzoyl-2′,3′-O-didecanoyl Guanosine ***8*** *(8Fc5Ph)*. Guanosine derivative **7** (54 mg, 0.07 mmol) was dried in vacuo over P_2O_5 at 50 °C for 2 h and then dissolved in DMF (1 mL). To the resulting solution were added Et_3N (15 μL, 0.10 mmol), benzoic anhydride (21 mg, 0.09 mmol), and a catalytic amount of DMAP. The mixture was stirred at room temperature for 8 h, and then, water (10 mL) and DCM (10 mL) were added. The organic phase was washed with water (10 mL), and the combined aqueous fractions were washed with DCM (2 × 5 mL). The organic fractions were combined, and solvents were removed under reduced pressure. The residue was purified by chromatography on silica (DCM/MeOH 96:4) to afford derivative **8** (52 mg, 0.06 mmol) as a yellow−orange solid in 85% yield.

RF = 0.13 (DCM/MeOH 96:4).

ESI-MS (m/z): 878.5 $[M - H]^-$; 880.4 $[M + H]^+$, 902.4 $[M + Na]^+$.

HRMS (ESI/Q-TOF) m/z: $[M + H]^+$ calcd for $C_{47}H_{62}FeN_5O_8$ 880.3942; found 880.3922.

^{1}H-NMR (CD_2Cl_2, 600 MHz): δ 12.40 (bs, 1H, NH), 7.92 (bd, 2H, ortho-Ph), 7.40 (bt, 1H, para-Ph), 7.31 (bt, 2H, meta-Ph), 6.90 (d, 1H, J = 3.8 Hz, H1'), 6.63 (dd, 1H, J = 5.7 Hz, 3.8 Hz, H2'), 5.51 (t, 1H, J = 5.7 Hz, H3'), 4.83−4.79 (m, 3H, H5', 2Fc), 4.58−4.54 (m, 2H, H4', H5'), 4.51 (bs, 1H, Fc), 4.48 (bs, 1H, Fc), 4.25 (s, 5H, Fc), 2.41−2.37 (m, 4H, 2 CH_2−CO), 1.69 (m, 2H, C$\underline{H}_2$−CH_2−CO), 1.62 (m, 2H, C$\underline{H}_2$−CH_2−CO), 1.39−1.21 (m, 24H, CH_2), 0.88 (t, 3H, CH_3), 0.85 (t, 3H, CH_3). $^{13}C\{^1H\}$ NMR (dmso-d_6, 151 MHz): δ 172.2 (CO), 172.2 (CO), 165.8 (CO), 158.5 (C), 153.5 (C), 152.4 (C), 146.1 (C), 133.9 (CH), 129.7 (C), 129.6 (CH), 128.1 (CH), 117.2 (C), 92.2 (CH), 86.7 (CH), 79.7 (C), 74.4 (CH), 71.0 (CH), 70.8 (CH), 69.9 (CH), 69.8 (CH), 68.7 (CH), 68.6 (CH), 63.5 (CH_2), 33.9 (CH_2), 33.6 (CH_2), 31.7 (CH_2), 31.7 (CH_2), 29.3 (CH_2), 29.2 (CH_2), 29.2 (CH_2), 29.1 (CH_2), 29.1 (CH_2), 28.9 (CH_2), 28.8 (CH_2), 24.8 (CH_2), 24.7 (CH_2), 22.5 (CH_2), 14.3 (CH_3).

https://doi.org/10.1021/acs.joc.1c00502
J. Org. Chem. 2021, 86, 9970−9978

■ ASSOCIATED CONTENT

Supporting Information

The Supporting Information is available free of charge at https://pubs.acs.org/doi/10.1021/acs.joc.1c00502.

Synthetic schemes, VT ^{1}H-NMR spectra, 1D-NOESY spectra, figures and tables, NMR spectra of compounds **1**−**14** (PDF)

■ AUTHOR INFORMATION

Corresponding Authors

Paolo Samorì − *Université de Strasbourg and CNRS, ISIS, Strasbourg 67000, France;* orcid.org/0000-0001-6256-8281; Email: samori@unistra.fr

Stefano Masiero − *Dipartimento di Chimica "Giacomo Ciamician", Alma Mater Studiorum−Università di Bologna, Bologna 40126, Italy;* orcid.org/0000-0001-6197-8297; Email: stefano.masiero@unibo.it

Authors

Marilena Campitiello − *Dipartimento di Chimica "Giacomo Ciamician", Alma Mater Studiorum−Università di Bologna, Bologna 40126, Italy*

Alessio Cremonini − *Dipartimento di Chimica "Giacomo Ciamician", Alma Mater Studiorum−Università di Bologna, Bologna 40126, Italy*

Marco A. Squillaci − *Université de Strasbourg and CNRS, ISIS, Strasbourg 67000, France*

Silvia Pieraccini − *Dipartimento di Chimica "Giacomo Ciamician", Alma Mater Studiorum−Università di Bologna, Bologna 40126, Italy*

Artur Ciesielski − *Université de Strasbourg and CNRS, ISIS, Strasbourg 67000, France;* orcid.org/0000-0003-3542-4092

Complete contact information is available at: https://pubs.acs.org/10.1021/acs.joc.1c00502

Funding

A. Ciesielski, P. Samorì, M. Campitiello and S. Masiero were financially supported by EC through the FP7 project ICT-MOLARNET (318516). A. Ciesielski, M.A. Squillaci, and P. Samorì were supported by the Marie Sklodowska-Curie ETN project SYNCHRONICS (GA 643238). S. Pieraccini, A. Cremonini, and S. Masiero were supported by the University of Bologna (RFO 2018 and RFO 2020). P. Samorì and A. Ciesielski were supported by the Labex projects CSC (ANR-10-LABX-0026 CSC) within the Investissement d'Avenir program ANR-10-IDEX-0002-02 and the International Center for Frontier Research in Chemistry (icFRC).

Notes

The authors declare no competing financial interest.

■ ACKNOWLEDGMENTS

We are grateful to Dr. Mohamed El Garah for enlightening discussions.

■ REFERENCES

(1) Stefan, L.; Monchaud, D. Applications of guanine quartets in nanotechnology and chemical biology. *Nat. Rev. Chem.* **2019**, *3*, 650−668.

(2) Davis, J. T.; Spada, G. P. Supramolecular architectures generated by self-assembly of guanosine derivatives. *Chem. Soc. Rev.* **2007**, *36*, 296−313.

(3) Arnal-Herault, C.; Pasc, A.; Michau, M.; Cot, D.; Petit, E.; Barboiu, M. Functional G-Quartet Macroscopic Membrane Films. *Angew. Chem., Int. Ed.* **2007**, *46*, 8409−8413.

(4) Yoshikawa, I.; Sawayama, J.; Araki, K. Highly Stable Giant Supramolecular Vesicles Composed of 2D Hydrogen-Bonded Sheet Structures of Guanosine Derivatives. *Angew. Chem., Int. Ed.* **2008**, *47*, 1038−1041.

(5) Sakaino, H.; Sawayama, J.; Kabashima, S.; Yoshikawa, I.; Araki, K. Dry Micromanipulation of Supramolecular Giant Vesicles on a Silicon Substrate: Highly Stable Hydrogen-Bond-Directed Nanosheet Membrane. *J. Am. Chem. Soc.* **2012**, *134*, 15684−15687.

(6) Ciesielski, A.; El Garah, M.; Masiero, S.; Samorì, P. Self-assembly of Natural and Unnatural Nucleobases at Surfaces and Interfaces. *Small* **2016**, *12*, 83−95.

(7) Sutyak, K. B.; Lee, W.; Zavalij, P. V.; Gutierrez, O.; Davis, J. T. Templating and Catalyzing [2+2] Photocycloaddition in Solution Using a Dynamic G-Quadruplex. *Angew. Chem., Int. Ed.* **2018**, *57*, 17146−17150.

(8) Lena, S.; Neviani, P.; Masiero, S.; Pieraccini, S.; Spada, G. P. Triggering of Guanosine Self-Assembly by Light. *Angew. Chem., Int. Ed.* **2010**, *49*, 3657−3660.

(9) Lena, S.; Masiero, S.; Pieraccini, S.; Spada, G. P. Guanosine Hydrogen-Bonded Scaffolds: A New Way to Control the Bottom-Up Realisation of Well-Defined Nanoarchitectures. *Chem. − Eur. J.* **2009**, *15*, 7792−7806.

(10) Ciesielski, A.; Lena, S.; Masiero, S.; Spada, G. P.; Samorì, P. Dynamers at the Solid−Liquid Interface: Controlling the Reversible Assembly/Reassembly Process between Two Highly Ordered Supramolecular Guanine Motifs. *Angew. Chem., Int. Ed.* **2010**, *49*, 1963−1966.

(11) Gonzalez-Rodriguez, D.; Janssen, P. G. A.; Martin-Rapun, R.; De Cat, I.; De Feyter, S.; Schenning, A. P. H. J.; Meijer, E. W. Persistent, Well-Defined, Monodisperse, π-Conjugated Organic Nanoparticles via G-Quadruplex Self-Assembly. *J. Am. Chem. Soc.* **2010**, *132*, 4710−4719.

(12) Rhodes, D.; Lipps, H. J. G-quadruplexes and their regulatory roles in biology. *Nucleic Acids Res.* **2015**, *43*, 8627−8637.

(13) Rivera, J. M. In *Guanine quartets: structure and application*, Fritzsche, W.; Spindler, L. Eds.; RSC Publishing, 2013; pp 15−27.

(14) Sutyak, K. B.; Zavalij, P. Y.; Robinson, M. L.; Davis, J. T. Controlling molecularity and stability of hydrogen bonded G-quadruplexes by modulating the structure's periphery. *Chem. Commun.* **2016**, *52*, 11112−11115.

(15) Martin-Hidalgo, M.; Garcia-Arriaga, M.; Gonzalez, F.; Rivera, J. M. Tuning supramolecular G-quadruplexes with mono- and divalent cations. *Supramol. Chem.* **2015**, *27*, 174−180.

(16) Marlow, A. L.; Mezzina, E.; Spada, G. P.; Masiero, S.; Davis, J. T.; Gottarelli, G. Cation-Templated Self-Assembly of a Lipophilic Deoxyguanosine: Solution Structure of a K^+−dG_8 Octamer. *J. Org. Chem.* **1999**, *64*, 5116−5123.

(17) Mezzina, E.; Mariani, P.; Itri, R.; Masiero, S.; Pieraccini, S.; Spada, G. P.; Spinozzi, F.; Davis, J. T.; Gottarelli, G. The Self-Assembly of a Lipophilic Guanosine Nucleoside into Polymeric Columnar Aggregates: The Nucleoside Structure Contains Sufficient Information To Drive the Process towards a Strikingly Regular Polymer. *Chem. − Eur. J.* **2001**, *7*, 388−395.

(18) Bare, G. A. L.; Liu, B.; Sherman, J. C. Synthesis of a Single G-Quartet Platform in Water. *J. Am. Chem. Soc.* **2013**, *135*, 11985−11989.

(19) El Garah, M.; Perone, R. C.; Santana-Bonilla, A.; Haar, S.; Campitiello, M.; Gutierrez, R.; Cuniberti, G.; Masiero, S.; Ciesielski, A.; Samori, P. Guanosine-based hydrogen-bonded 2D scaffolds: metal-free formation of G-quartet and G-ribbon architectures at the solid/liquid interface. *Chem. Commun.* **2015**, *51*, 11677−11680.

(20) Inui, Y.; Shiro, M.; Fukuzumi, S.; Kojima, T. Quartet formation of a guanine derivative with an isopropyl group: crystal structures of "naked" G-quartets and thermodynamics of G-quartet formation. *Org. Biomol. Chem.* **2013**, *11*, 758−764.

(21) Sessler, J. L.; Sathiosatham, M.; Doerr, K.; Lynch, V.; Abboud, K. A. A G-Quartet Formed in the Absence of a Templating Metal Cation: A New 8-(N,N-dimethylaniline)guanosine Derivative. *Angew. Chem., Int. Ed.* **2000**, *39*, 1300−1303.
(22) Murat, P.; Gennaro, B.; Garcia, J.; Spinelli, N.; Dumy, P.; Defrancq, E. The Use of a Peptidic Scaffold for the Formation of Stable Guanine Tetrads: Control of a H-bonded Pattern in Water. *Chem. − Eur. J.* **2011**, *17*, 5791−5795.
(23) Nikan, M.; Sherman, J. C. Cation-Complexation Behavior of Template-Assembled Synthetic G-Quartets. *J. Org. Chem.* **2009**, *74*, 5211−5218.
(24) Masiero, S.; Trotta, R.; Pieraccini, S.; De Tito, S.; Perone, R.; Randazzo, A.; Spada, G. P. A non-empirical chromophoric interpretation of CD spectra of DNA G-quadruplex structures. *Org. Biomol. Chem.* **2010**, *8*, 2683−2692.
(25) Claridge, T. D. V. *High-Resolution NMR Techniques in Organic Chemistry*, 3rd ed.; Pergamon-Elsevier, Oxford, 1999.
(26) Buerkle, L. E.; von Recumab, H. A.; Rowan, S. J. Toward potential supramolecular tissue engineering scaffolds based on guanosine derivatives. *Chem. Sci.* **2012**, *3*, 564−572.
(27) Kotch, F. W.; Sidorov, V.; Lam, Y.-F.; Kayser, K. J.; Li, H.; Kaucher, M. S.; Davis, J. T. Water-Mediated Association Provides an Ion Pair Receptor. *J. Am. Chem. Soc.* **2003**, *125*, 15140−15150.
(28) Liscio, A.; Palermo, V.; Samorì, P. Probing Local Surface Potential of Quasi-One-Dimensional Systems: A KPFM Study of P3HT Nanofibers. *Adv. Funct. Mater.* **2008**, *18*, 907−914.
(29) Ciuchi, F.; Dinicola, G.; Franz, H.; Gottarelli, G.; Mariani, P.; Bossi, M. G. P.; Spada, G. P. Self-Recognition and Self-Assembly of Folic Acid Salts: Columnar Liquid Crystalline Polymorphism and the Column Growth Process. *J. Am. Chem. Soc.* **1994**, *116*, 7064−7071.
(30) Hobza, P.; Šponer, J. Structure, Energetics, and Dynamics of the Nucleic Acid Base Pairs: Nonempirical Ab Initio Calculations. *Chem. Rev.* **1999**, *99*, 3247−3276.
(31) De Luca, G.; Liscio, A.; Maccagnani, P.; Nolde, F.; Palermo, V.; Müllen, K.; Samorì, P. Nucleation-Governed Reversible Self-Assembly of an Organic Semiconductor at Surfaces: Long-Range Mass Transport Forming Giant Functional Fibers. *Adv. Funct. Mater.* **2007**, *17*, 3791−3798.
(32) Kim, D. H.; Lee, D. Y.; Lee, H. S.; Lee, W. H.; Kim, Y. H.; Han, J. I.; Cho, K. High-Mobility Organic Transistors Based on Single-Crystalline Microribbons of Triisopropylsilylethynyl Pentacene via Solution-Phase Self-Assembly. *Adv. Mater.* **2007**, *19*, 678−682.
(33) De Luca, G.; Liscio, A.; Nolde, F.; Scolaro, L. M.; Palermo, V.; Müllen, K.; Samorì, P. Self-assembly of discotic molecules into mesoscopic crystals by solvent-vapour annealing. *Soft Matter* **2008**, *4*, 2064−2070.
(34) El Garah, M.; Bonilla, A. S.; Ciesielski, A.; Gualandi, A.; Mengozzi, L.; Fiorani, A.; Iurlo, M.; Marcaccio, M.; Gutierrez, R.; Rapino, S.; Calvaresi, M.; Zerbetto, F.; Cuniberti, G.; Cozzi, P. G.; Paolucci, F.; Samorì, P. Molecular design driving tetraporphyrin self-assembly on graphite: a joint STM, electrochemical and computational study. *Nanoscale* **2016**, *8*, 13678−13686.
(35) Gillet, L. C. J.; Schärer, O. D. Preparation of C8-Amine and Acetylamine Adducts of 2′-Deoxyguanosine Suitably Protected for DNA Synthesis. *Org. Lett.* **2002**, *4*, 4205−4208.

https://doi.org/10.1021/acs.joc.1c00502
J. Org. Chem. 2021, 86, 9970−9978